BIOCHEMISTRY
including biophysical chemistry & molecular biology

Article

pubs.acs.org/biochemistry

Transient Non-Native Burial of a Trp Residue Occurs Initially during the Unfolding of a SH3 Domain

Amrita Dasgupta and Jayant B. Udgaonkar*

National Centre for Biological Sciences, Tata Institute of Fundamental Research, Bangalore 560065, India

ABSTRACT: The detection and characterization of non-native interactions in a partially unfolded form of any protein are important not only with regard to how they might facilitate folding but also in the context of their possible role in driving the protein toward amyloid fibril formation. The SH3 domain of PI3 kinase is known to unfold via an early, partially unfolded intermediate. In this study, the kinetics of unfolding of this protein in guanidine hydrochloride was studied by monitoring the fluorescence of its sole tryptophan residue, W53. W53 is fully solvent-exposed in both the native and unfolded states, as indicated by a similar wavelength (356−357 nm) of maximal fluorescence emission, and a similar quantum yield of fluorescence. W53 becomes partially buried in the unfolding intermediate, as seen in the 6−7 nm blue shift in its wavelength of maximal fluorescence emission in the intermediate, and in the transient initial increase in the quantum yield of its fluorescence during unfolding. It appears that W53 is engaged in non-native interactions in the unfolding intermediate. It is also shown that the transition from the native state to the unfolding intermediate occurs as a gradual and not an all-or-none transition.

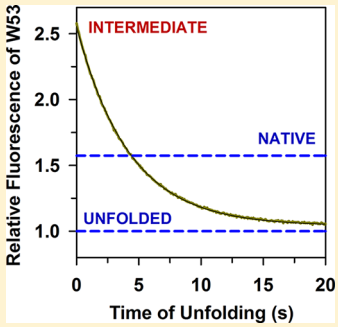

The unfolded states of many proteins have been shown to possess specific stabilizing interactions not present in the folded states.[1−6] Such non-native interactions may persist, or new non-native interactions may form, when the unfolded protein becomes compact upon being transferred to refolding conditions.[2,7,8] It also appears that native-like structure may be stabilized by non-native interactions in compact unfolded states.[6,9−11] Non-native structure has also been detected in molten globules populated at equilibrium,[12,13] as well as in kinetic folding intermediates,[8,14−23] where they may play a role in accelerating the folding reaction.[24] φ value analysis of the transition-state (TS) ensemble[25] has had a dominant role in experimental studies of protein folding, and noncanonical φ values[26,27] as well as high canonical φ values[28] have been interpreted in terms of non-native contacts in the TS. Residues that have been identified in this way to make key non-native interactions in the TS appear to be important in determining folding kinetics rather than native-state stability.[29]

Evidence that non-native interactions may play a productive role in protein folding is at odds with native-centric views of folding.[30] Native-centric views of folding originated from simplified computational studies based on the Gō model,[31] in which interactions present only in the native state are incorporated. They have been reinforced by experimental studies that suggest that the TSs of folding of apparently two-state folding proteins[32] have native-like topology.[33] While it remains difficult to detect experimentally the formation of non-native structures on protein folding pathways,[34] dissatisfaction with the native-centric view[34−36] has led to the development of computational models in which the protein samples both native and non-native conformations during the folding/unfolding process.[30,37−40]

It is especially important to determine how late into the folding process non-native interactions persist. One way of studying structures formed after the rate-limiting step of folding is to study the unfolding reaction, both under native conditions and under unfolding conditions. Native-state hydrogen exchange (HX) studies have provided much information about partially folded forms populated before the rate-limiting step of unfolding, and presumably after the rate-limiting step of folding,[41−43] but HX is not suited to identifying non-native interactions. Partly unfolded intermediates have also been detected in kinetic studies that show that they are often populated early during unfolding,[42,44−50] and for some proteins, they may possess non-native interactions.[18,48,51]

Kinetic unfolding studies performed on the SH3 domain of the PI3 kinase (PI3K SH3), at low and high concentrations of guanidine hydrochloride (GdnHCl), have revealed that unfolding intermediate ensembles, I_N and I_U, are populated very early during unfolding.[43,50] I_U possesses native-like secondary structure and U-like tyrosine (Tyr) fluorescence, highlighting its molten globule-like properties, and is populated at very high concentrations of GdnHCl.[50] I_N has N-like fluorescence, but unlike N, it has two loops showing U-like protection against hydrogen exchange and is populated only in the absence of GdnHCl or in the presence of low concentrations of GdnHCl.[43] There is no evidence, from native-state hydrogen exchange studies, of any U being populated in the absence of GdnHCl.[43] Amyloid fibril formation by the PI3K SH3 domain has been studied extensively,[52,53] but identification of the monomeric form from which such aggregation commences remains elusive.

In this study, the unfolding of the PI3K SH3 domain in GdnHCl was investigated using the fluorescence of the sole Trp

Received: June 27, 2012
Revised: August 28, 2012
Published: September 21, 2012

residue, W53, as well as ANS fluorescence as the probes. The native (N) and unfolded (U) states are shown to have similar quantum yields of intrinsic Trp fluorescence, and the equilibrium unfolding transition appears to be anomalous when measured by this probe. W53 is shown to be fully solvent-exposed in the native state (N) of the protein (Figure 1), and

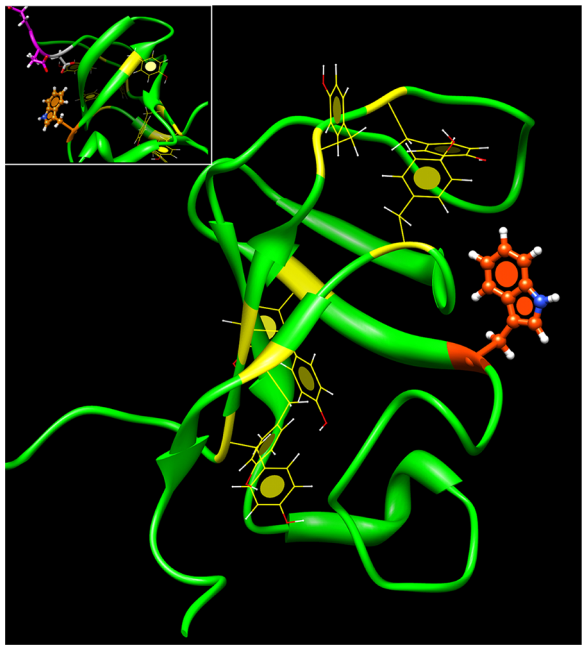

Figure 1. Structure of the PI3K SH3 domain showing the single Trp residue (red), W53, and the seven Tyr residues (yellow) at positions 4, 6, 10, 12, 57, 71, and 74. The NH group of the side chain of W53 is seen to be oriented toward the solvent and away from the π-clouds of all the Tyr residues. The inset shows the arrangement of Glu17 (magenta), Glu18 (magenta), and Asp19 (gray) with respect to W53 in the vicinity of W53. The ribbon diagram was generated from Protein Data Bank entry 1pnj using the UCSF Chimera package from the Resource for Biocomputing, Visualization, and Informatics at the University of California, San Francisco.[85]

the native and unfolded (U) states have similar Trp fluorescence. Nevertheless, in kinetic studies, a transient burst phase increase in Trp fluorescence is observed to accompany the formation of I_U during unfolding at high denaturant concentrations, which increases in a monotonically linear manner with an increase in the concentration of the denaturant in which the protein is unfolded. A transient increase in ANS fluorescence is also observed, indicating that I_U has features of a wet molten globule. Thus, it is shown that the unfolding of the PI3K SH3 domain proceeds via the transient, partial, and non-native burial of W53 in a molten globule intermediate, I_U.

MATERIALS AND METHODS

Protein Expression and Purification. The protein was purified as described previously.[50,54] Electrospray ionization mass spectrometry showed that the protein had the expected mass of 9276.2 Da.

Buffers, Reagents, and Experimental Conditions. All reagents and buffers of the highest purity were procured from Sigma. Ultrapure grade GdnHCl was obtained from USB Corp. Phosphate buffer (20 mM, pH 7.2) was included in the buffers used for all experiments, which were all performed at 25 °C. NATA (*N*-acetyl-L-tryptophanamide) of the highest purity was procured from Sigma. The concentrations of stock solutions of GdnHCl were determined by refractive index measurements on an Abbe refractometer. The concentration of the protein was determined by measurement of absorbance at 280 nm using an ε of 17900 M^{-1} cm^{-1}.[55]

For equilibrium unfolding experiments using Trp fluorescence as the probe, the protein concentrations were 10−15 μM. For the kinetic unfolding experiments, using Trp fluorescence, the protein concentration was 20 μM.

Equilibrium Unfolding Experiments. Fluorescence experiments were performed on a stopped-flow module (SFM-4, Biologic) in a fluorescence cuvette with a path length of 1 cm. The wavelength used for the selective excitation of Trp fluorescence was 295 nm, with a bandwidth of 4 nm. The fluorescence emission was measured through either a 320 nm (Asahi Spectra) or a 387 nm (Semrock) band-pass filter with a bandwidth of 10 nm.

Kinetic Unfolding Experiments. All kinetic unfolding experiments, using either Trp fluorescence or ANS fluorescence as the probe, were performed using the SFM-4 stopped-flow module. Typically, a dead time of 6 ms was achieved with a cuvette with a path length of 0.15 cm. For experiments using ANS, the ANS concentration was 540 μM in the unfolding buffer and the protein concentration was 45 μM. The wavelength for excitation was 295 nm with a bandwidth of 4 nm, and the emission wavelength was 450 nm with a bandwidth of 25 nm.

To obtain a spectrum of the protein at time zero, kinetic traces of unfolding in 3.7 M GdnHCl were monitored at different emission wavelengths, with fluorescence excitation at 295 nm. For this purpose, a stopped-flow module (RX2000 rapid kinetic spectrometer accessory from Applied Photophysics) was synchronized with a Spex Fluoromax 3 spectrofluorimeter. A dead time of 60 ms was achieved with a 1:5 ratio of mixing: 160 μL of native protein was diluted into 640 μL of 4.6 M GdnHCl. The single-exponential fits to the kinetic traces were extrapolated to time zero to obtain the spectrum at time zero.

RESULTS

Spectroscopic Characterization of the PI3K SH3 Domain by Fluorescence Measurements. In this study, the unfolding of the PI3K SH3 domain has been investigated by utilizing intrinsic Trp fluorescence as the probe for the first time. Previous studies of unfolding had utilized measurements of intrinsic tyrosine fluorescence.[50,54] Panels A and B of Figure 2 show the fluorescence spectra of the protein when it is excited at 268 nm, upon which both Tyr and Trp fluorescence is excited, and when the protein is excited at 295 nm, only Trp fluorescence is excited. Upon excitation at 268 nm, the fluorescence spectrum of the protein shows an emission maximum at 356 nm, with a small shoulder at 300 nm (Figure 2A).[54] Tyr fluorescence is quenched by the sole Trp residue (W53). The extent of this quenching is higher in N than in U in 4 M GdnHCl.

When the excitation wavelength is, however, 295 nm, the fluorescence spectra obtained for N and for U in 4 M GdnHCl indicate that the quantum yields of W53 fluorescence, as given by the areas under the spectra, are the same in states N and U. The similar quantum yields of fluorescence in N and U indicate that there is no additional mechanism for the quenching of W53 fluorescence in N that is absent in U, and that the fluorescence of W53 is as much quenched by solvent in N as it

dx.doi.org/10.1021/bi3008627 | *Biochemistry* 2012, 51, 8226−8234

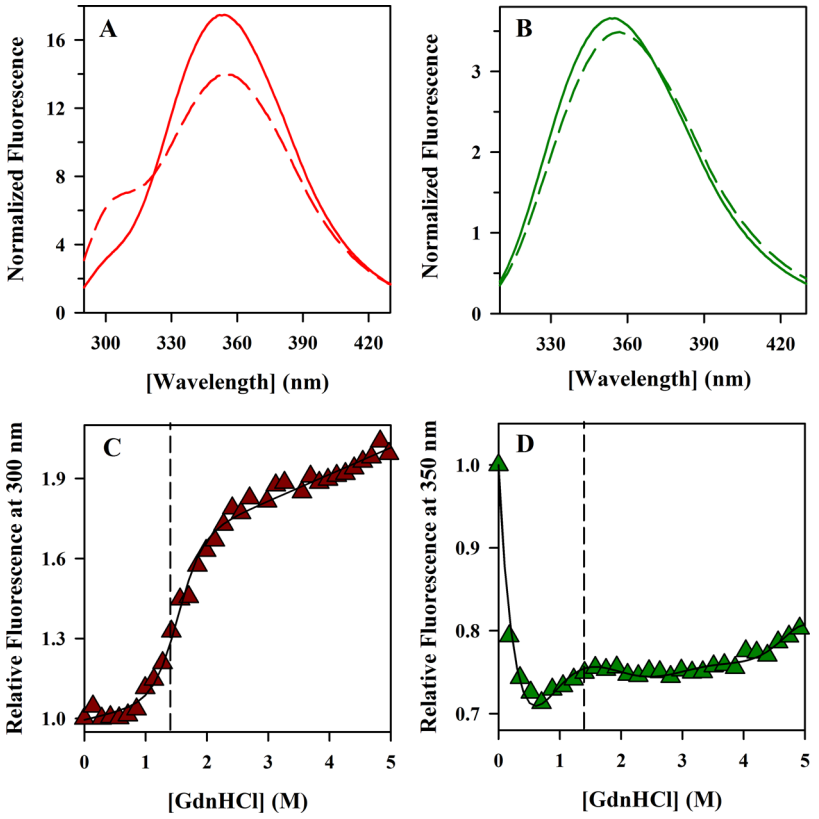

Figure 2. Fluorescence emission spectra and equilibrium unfolding curves of the PI3K SH3 domain. Fluorescence emission spectra with excitation at 268 (A) and 295 nm (B). The solid lines in all panels represent the spectra of the native state in zero denaturant. The dashed lines in panels A and B show the spectra of the unfolded state in 4 M GdnHCl. Each spectrum in panels A and B was normalized to a value of 1 for the fluorescence signal at 320 nm of the unfolded protein upon excitation at 295 nm. Panel C shows an equilibrium unfolding transition of the PI3K SH3 domain monitored by measurement of tyrosine fluorescence at 300 nm upon excitation at 268 nm. Panel D shows an equilibrium unfolding transition of the protein monitored by measurement of W53 fluorescence at 350 nm upon excitation at 295 nm. The fluorescence data in panels C and D have been normalized to a value of 1 for the native state in each case. The solid line through the data in panel C is a fit to a two-state N ↔ U model, with values for the free energy of unfolding and the midpoint of the transition of 4.2 kcal mol^{-1} and 1.4 M, respectively. The vertical dashed lines in panels C and D indicate the value of 1.4 M for C_m. The solid line through the data in panel D was drawn by inspection only.

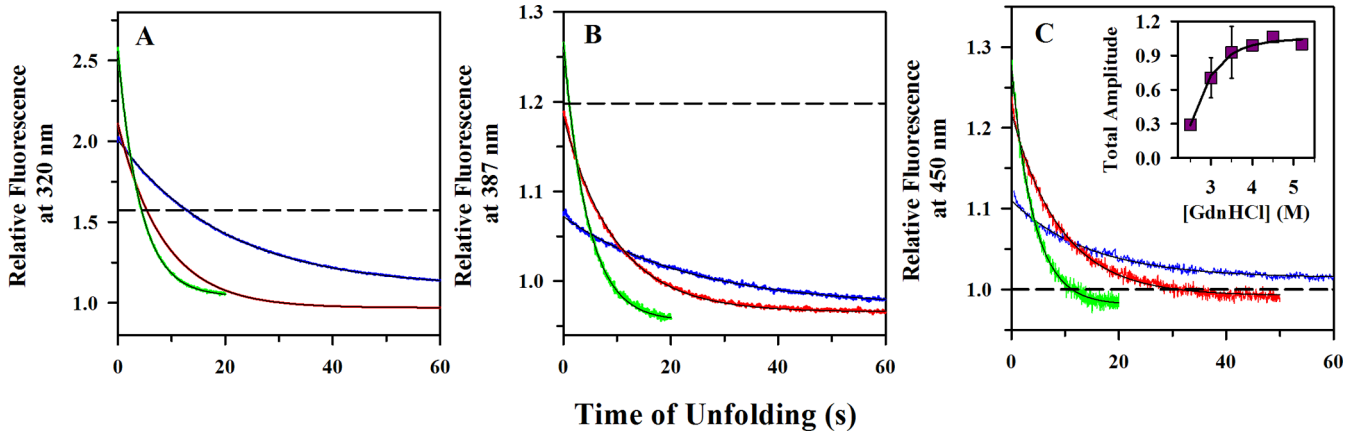

Figure 3. Kinetic traces of unfolding of the PI3K SH3 domain at pH 7.2 and 25 °C. Unfolding in GdnHCl was probed by measurement of the change in the intrinsic Trp fluorescence signal at 320 (A) and 387 nm (B), as well as of the change in ANS fluorescence at 450 nm with an excitation at 295 nm (C). The data in panels A–C were obtained when the native protein was diluted into 2.5 (blue), 3 (red), and 3.5 M GdnHCl (green). In panels A and B, each trace was normalized to a value of 1 for the fluorescence signal of the unfolded protein in 4 M GdnHCl. In panel C, each trace was normalized to a value of 1 for the fluorescence signal of the native protein. The inset in panel C shows the dependence of the total amplitude of the ANS fluorescence change (maroon squares) on the concentration of GdnHCl present during unfolding. The amplitudes are normalized to a value of 1 for the amplitude of the ANS fluorescence change observed for unfolding in 5.3 M GdnHCl. The dashed lines in panels A and B represent the fluorescence signal of the native protein. In all the panels, the solid lines through the traces represent fits to a single-exponential equation. The error bars represent standard deviations obtained from two independent experiments.

dx.doi.org/10.1021/bi3008627 | *Biochemistry* 2012, 51, 8226–8234

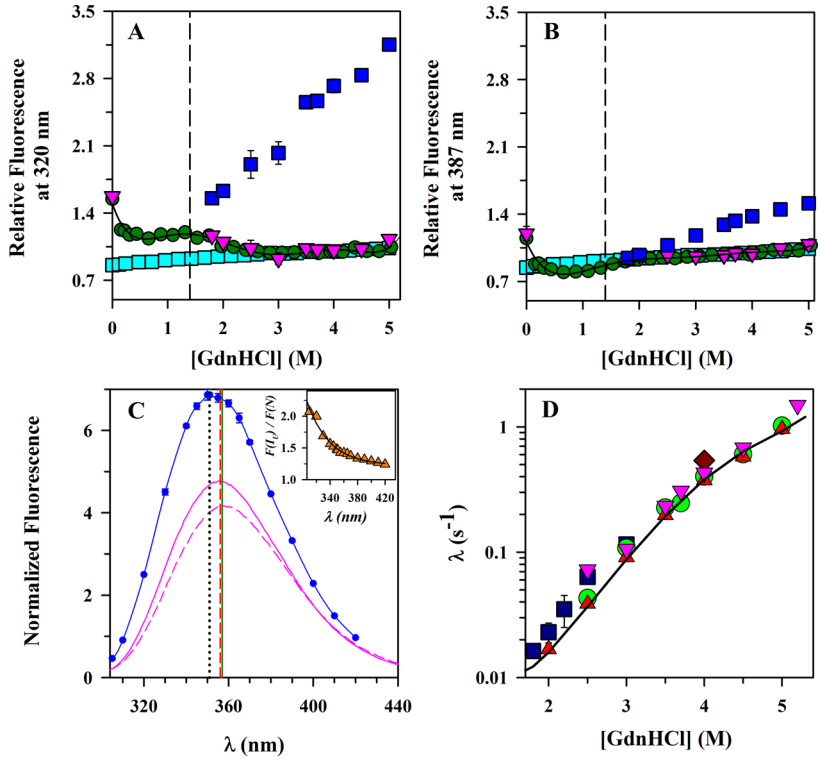

Figure 4. Kinetics of GdnHCl-induced unfolding monitored by Trp and ANS fluorescence. Panels A and B show the equilibrium vs kinetic amplitudes of unfolding monitored using the fluorescence of W53 at 320 and 387 nm, respectively, upon excitation at 295 nm: (green circles) the equilibrium unfolding transition of the protein, (blue squares) time zero points, and (magenta triangles) $t = \infty$ points of the kinetic traces of unfolding. The solid lines through the equilibrium points (green circles) for unfolding in panels A and B were drawn by inspection only. The vertical dashed lines in panels A and B represent the positions of the midpoint (C_m = 1.4 M) of the equilibrium unfolding transition, determined from the experiment in Figure 2C. Also shown in panels A and B are the dependencies of the fluorescence of NATA (turquoise squares) upon excitation at 295 nm, when measured at 320 (A) and 387 nm (B). In each of the panels, the fluorescence of the protein was normalized to a value of 1 for the fluorescence in 4 M GdnHCl. Similarly, the fluorescence values of NATA in different GdnHCl concentrations were normalized to a value of 1 for NATA in 4 M GdnHCl. Panel C shows the fluorescence emission spectra, upon excitation at 295 nm, of the N state (solid pink line), the U form in 3.7 M GdnHCl (dashed pink line), and the initial burst phase product (I_U) at 0 ms of unfolding in 3.7 M GdnHCl (blue circles). Each spectrum in panel C was normalized to a value of 1 for the fluorescence signal at 320 nm of the unfolded protein in 3.7 M GdnHCl. The dotted line shows the λ_{max} for the initial burst phase product (I_U) at 0 ms of unfolding in 3.7 M GdnHCl; the dashed line shows the λ_{max} for the N state, and the solid line shows the λ_{max} for the U state in 3.7 M GdnHCl. The inset in panel C shows the dependence of the ratio of the fluorescence of the burst phase intermediate [$F(I_U)$] to that of the N state [F(N)] at different wavelengths of emission. The solid line in the inset was drawn by inspection only. Panel D shows the comparison of the observed rates of unfolding using (dark blue squares) the intrinsic Tyr fluorescence at 300 nm,[50] (red triangles and green circles) Trp fluorescence at 320 and 387 nm, respectively, and (magenta triangles) ANS fluorescence at 450 nm in GdnHCl as the probes. The brown diamond represents the observed rate of unfolding for a 15-fold higher concentration of protein, determined by measurement of W53 fluorescence at 387 nm at 4 M GdnHCl. The solid line through the data in panel D indicates the fit to the three-state model for unfolding described previously.[50] The error bars represent standard deviations obtained from two independent experiments.

is in U. Indeed, examination of the structure of the vicinity of W53 in N indicates that the side chain of W53 is oriented such that it would be minimally quenched by neighboring Tyr residues, or by any neighboring Glu or Asp residues (Figure 1).

The wavelength of maximal fluorescence emission upon excitation at 295 nm is seen to be approximately the same in N and U: it is at 356 nm for N and 357 nm for U (Figure 2B). This indicates that W53 is as solvent-exposed in N as it is in U. Although calculations of solvent-accessible surface area indicate that the side chain of W53 has a surface accessibility of only 60% (computed using the algorithm in ref 56), the U-like solvent exposure of W53 in N was confirmed by acrylamide quenching experiments, which indicate that the bimolecular quenching rate constant, k_q, has the same near diffusion-controlled value in states N and U (M. Kishore and J. B. Udgaonkar, unpublished results).

Figure 2C shows an equilibrium unfolding curve of the protein determined by monitoring Tyr fluorescence at 300 nm, the wavelength at which the spectra of N and U are most different (Figure 2A). Because the protein contains seven Tyr residues distributed throughout the sequence, the sigmoidal transition curve, characteristic of a two-state N ↔ U transition, monitors the loss of tertiary interactions globally throughout the protein.[50] Figure 2D shows the equilibrium unfolding transition determined by measurement of W53 fluorescence emission at 350 nm, the wavelength of maximal emission, on GdnHCl concentration. The transition induced by GdnHCl is anomalous and not characteristic of a typical two-state transition. In contrast, the equilibrium transition induced by urea is sigmoidal in nature.[54]

Millisecond Measurements of the Kinetics of Unfolding Monitored by the Measurement of the Fluorescence of W53 and ANS Fluorescence. Panels A and B of Figure 3 show representative kinetic traces of unfolding probed by the measurement of W53 fluorescence at 320 and 387 nm, respectively. In both instances, the kinetic traces of unfolding

dx.doi.org/10.1021/bi3008627 | Biochemistry 2012, 51, 8226−8234

(in >2 M GdnHCl at 320 nm and in >3.5 M GdnHCl at 387 nm) do not extrapolate to the value of the fluorescence of the native protein, but to fluorescence values exceeding the native-state fluorescence. This result suggests that the burst phase intermediate, I_U, which was previously identified,[50] has Trp fluorescence properties that are different from those of N and U. Unfolding subsequent to this burst phase occurs in a single-exponential phase at all GdnHCl concentrations.

The hydrophobic dye, ANS, binds to solvent-exposed hydrophobic clusters on proteins.[57] This binding results in an increase in the fluorescence quantum yield of the dye, and in a blue shift in the fluorescence spectrum. Figure 3C shows that when unfolding is conducted in the presence of ANS, there is a burst phase increase in ANS fluorescence, within the dead time of stopped-flow mixing (6 ms). This initial jump in ANS fluorescence is relatively small and corresponds to an increase of only 20−30% of the ANS fluorescence of the unfolded protein. Subsequently, a decrease in ANS fluorescence is observed, as the protein completely unfolds, and this decrease occurs in a single kinetic phase at all GdnHCl concentrations. The inset in Figure 3C shows that the amplitude of the burst phase increase in ANS fluorescence becomes larger with an increase in GdnHCl concentration.

Panels A and B of Figure 4 compare the equilibrium and kinetic amplitudes of W53 fluorescence-monitored unfolding in GdnHCl at 320 and 387 nm, respectively. The change in the Trp fluorescence of the protein, at either 320 or 387 nm, observed in the equilibrium unfolding transitions, is small and is comparable in magnitude to that seen for NATA with an increase in denaturant concentration, as shown in panels A and B of Figure 4. The fluorescence emission at 320 and 387 nm shows no change when the protein goes from low to high concentrations of GdnHCl, as expected for a Trp residue that is exposed in both N and U. Because the changes in Trp fluorescence at 320 and 387 nm in the equilibrium unfolding transitions were negligible, clear native and unfolded protein baselines were not observed. Nevertheless, it is seen that the fluorescence signals at the time zero points of the kinetic traces of unfolding above 2.5 M GdnHCl, which represent the fluorescence of W53 in I_U, lie above the fluorescence signal expected for fully exposed W53 in the native or unfolded protein. The fluorescence of W53 has a much stronger dependence on GdnHCl concentration in I_U than in N or U, and this dependence is much stronger than that of NATA. Thus, the amplitude of the burst phase change in the fluorescence of W53 increases with an increase in GdnHCl concentration, and the amplitude at any concentration of GdnHCl is higher at 320 nm than at 387 nm (Figure 4A,B). The data in panels A and B of Figure 4 also show that the $t = \infty$ points of the kinetic traces of unfolding lie on the equilibrium unfolding transitions, indicating that all reactions were monitored to completion.

The data therefore suggested that the fluorescence spectrum of W53 in I_U might be blue-shifted not only with respect to that of W53 in U, as has been reported for Trp residues that are partially buried in the folding intermediates of other proteins,[58−60] but also with respect to that of W53 in N. Hence, the Trp fluorescence spectrum of I_U, upon excitation at 295 nm, was determined. Figure 4C compares the fluorescence emission spectrum of I_U in 3.7 M GdnHCl to the spectrum of N, and to the spectrum of U in 3.7 M GdnHCl. The spectrum for I_U has an emission maximum at 350 nm, which is blue-shifted by ∼6 nm from the emission maximum at 356 nm for N and by ∼7 nm from the emission maximum at 357 nm for U in 3.7 M GdnHCl. The spectrum of I_U also indicates that the quantum yield of W53 is significantly higher in I_U than it is in N and U. The inset in Figure 4C shows that the relative increase in Trp fluorescence upon the formation of I_U is greater at lower wavelengths on the blue side of the fluorescence emission spectrum of N and decreases with an increase in wavelength on the red side of the spectrum.

Multiple Spectroscopic Probes Monitor the Same Unfolding Pathway. Figure 4D shows a comparison of the observed rates of unfolding monitored using intrinsic Tyr fluorescence,[50] Trp fluorescence at 320 and 387 nm, and ANS fluorescence at 450 nm. At any GdnHCl concentration, the observed unfolding rate constants measured by the different probes are identical. In previous studies,[50,61] the kinetics of unfolding at GdnHCl concentrations above 3 M were immeasurable because the entire intrinsic Tyr fluorescence change occurred within the dead time of mixing.[50] It is observed here, using Trp fluorescence and ANS fluorescence as the probes, that the observed rates of unfolding can be measured reliably above 3 M GdnHCl. Moreover, the curvature in the unfolding arm of the chevron becomes clear when it is constructed with rate constants monitored by Trp fluorescence and ANS fluorescence. To rule out the possibility of transient aggregation, we monitored unfolding of a 15-fold higher concentration of the protein in 4 M GdnHCl by measuring the W53 fluorescence at 387 nm. It is seen that the rate of unfolding remains unchanged (Figure 4D).

The data in Figure 4D were fit to the three-state model (N ↔ I_U ↔ U) described in detail previously.[50] The parameters used to fit the observed data were identical to those obtained in the previous study.

DISCUSSION

Structural Features of the Early Unfolding Intermediate, I_U. The unfolding mechanism of the PI3K SH3 domain in the presence of high concentrations of denaturant was shown earlier to proceed via a three-state mechanism, with an on-pathway unfolding intermediate (I_U) forming early during unfolding.[50] Further studies in the presence of a stabilizing cosolute, Na_2SO_4, indicated that I_U was stabilized to the same extent as the native state.[62] In both studies, I_U manifested itself as a very early unfolding intermediate, whose formation was accompanied by a burst phase change in the intrinsic Tyr fluorescence of the protein, and whose accumulation resulted in a downward curvature being observed in the unfolding arm of the chevron plot. It was concluded from the study in the absence of salt that I_U has U-like tyrosine fluorescence properties, but N-like far-UV CD properties.[50] In this study (Figure 3C), it is shown that I_U binds to the hydrophobic dye, ANS, albeit weakly, suggesting that it possesses a solvent-accessible hydrophobic surface. Hence, I_U appears to possess the classical features of a molten globule intermediate.[63]

The formation of solvent-accessible surface area in I_U would have come at the expense of considerable loosening of structure, but it is not known at present whether water molecules are able to penetrate the hydrophobic core in I_U, as has been suggested for molten globules in general.[64] A thermodynamic analysis of the N ↔ I_U transition has, however, indicated that I_U possesses ∼45% of the solvent-accessible surface area present in U, suggesting that considerable water penetration has occurred in I_U.[50] The PI3K SH3 domain has seven Tyr residues distributed throughout the molecule (Figure

dx.doi.org/10.1021/bi3008627 | Biochemistry 2012, 51, 8226−8234

1), and the observation[50,54] that the tyrosine fluorescence of I_U is U-like also suggests that considerable penetration of water has occurred in I_U.

The extent to which I_U is populated at the end of the burst phase of unfolding increases as the GdnHCl concentration is increased to ~3 M.[50] The observed increase in the amplitude of the burst phase increase in ANS fluorescence (Figure 3C, inset) would represent the increase in the extent to which I_U is populated at the end of the burst phase. Above ~3 M GdnHCl, I_U is fully populated at the end of the burst phase of unfolding.[50] Nevertheless, the amplitude of the burst phase change in ANS fluorescence continues its monotonic increase with an increase in GdnHCl concentration even at GdnHCl concentrations above 3 M and saturates above 4 M. This indicates that the extent of solvent-accessible hydrophobic surface competent to bind ANS increases in I_U with an increase in GdnHCl concentration. It therefore appears that complete disruption of internal packing and consequent generation of hydrophobic surface in I_U occurs gradually in a nonsigmoidal fashion as the GdnHCl concentration is increased.

Hyperfluorescence of W53 in I_U Is Not Due to the Release of Quenching Present in N. It is possible that even minor structural perturbations due to the addition of GdnHCl would be sufficient to alter specific tertiary interactions in I_U,[65,66] and this could lead to a change in the arrangement of local quenching groups in the vicinity of W53. Hence, a relatively trivial reason for the transient initial increase in the fluorescence of W53 during unfolding could be that the fluorescence of W53 is quenched in the native protein, and that this quenching is released immediately when unfolding commences. But the observation that the quantum yield of fluorescence of W53 in N is the same as in U (see Results) strongly indicates that the fluorescence of W53 in N is not quenched by any part of the structure of N. If the fluorescence of W53 is at all quenched in N, it is quenched by water to the same extent as it is quenched in U. Moreover, an examination of the structure of the protein (Figure 1) suggests that this is very unlikely. If the fluorescence of W53 is quenched in N, it would have to be by the Tyr residues, because nearby Glu and Asp residues would be deprotonated at pH 7.2 and, hence, would not be able to act as quenchers.[67] A Tyr residue cannot quench the fluorescence of a Trp residue by fluorescence resonance energy transfer, because of the negligible overlap between the emission spectrum of a Trp and the absorption spectrum of a Tyr residue.[68] A Tyr residue can also quench the fluorescence of a Trp residue by excited-state proton transfer, but only when the NH group of the indole ring of the latter is oriented such that it can interact with the π-cloud of the former.[67,69] The NH group of the indole ring of W53 is completely solvent-exposed (Figure 1) and is not in a favorable orientation for interacting with the π-cloud of any of the Tyr residues. Hence, the hyperfluorescence of I_U cannot be attributed to the release of fluorescence quenching that was present in N.

Partial Burial of W53 in I_U. The other reason for the hyperfluorescence of W53 in I_U could be that W53, which is as fully solvent-exposed in N as it is in U (see Results), becomes partially buried in I_U. Such an inference is supported by the observation that the fluorescence spectrum of W53 in I_U is blue-shifted by ~6 nm (Figure 4C) with respect to the spectra of W53 in N and U. It is well-known that Trp residues in a protein exhibit blue shifts in their fluorescence emission wavelength maxima, depending on the extent of exposure to water.[69] The observation of a blue shift of only ~6 nm suggests either that W53 has become fully buried in only a fraction of the protein molecules, or more likely that I_U is an ensemble of molecules in which W53 is buried to different extents. The observation that the relative increase in the fluorescence of W53 in I_U over that in N is more on the blue side of the fluorescence emission spectrum than on the red side (Figure 4C, inset) supports the latter possibility. The observation that the fluorescence intensity of W53 in I_U is significantly higher at 320 nm (Figure 4A), while it is marginally higher at 387 nm than at 320 nm in N and U (Figure 4B), supports the conclusion that W53 is partially buried in I_U.

The fluorescence of W53, unlike that of the seven Tyr residues, provides site-specific information at the residue level about the nature of tertiary contacts initiated or disrupted initially during structure dissolution. W53 is positioned at the beginning of the third β-strand (Figure 1). The binding of ANS to I_U already suggests that the hydrophobic core packing has loosened, and therefore, it may be possible that this loosening leads to a cavity where the conformationally flexible Trp residue is temporarily buried and is shielded from the effects of solvent quenching. Because I_U possesses a hydrophobic surface capable of binding to ANS (see above), it would appear that W53 might be participating in the formation of such a hydrophobic surface. It appears therefore that W53 must be engaged in non-native long-range interactions with other neighboring residues in order to bury itself in a hydrophobic pocket.

Nature of the Transition from N to I_U. Several studies have indicated that the initial collapse of the protein chain during protein folding may be a gradual process that is slowed by many distributed, small free energy barriers instead of one dominant free energy barrier.[54,70−75] This study suggests that the initial step in the unfolding of the PI3K SH3 domain, leading to the transient non-native burial of W53 in I_U, may likewise be a gradual process and not an all-or-none, cooperative process: the burst phase increases in W53 hyperfluorescence (Figure 4A,B) and ANS fluorescence (Figure 3C, inset) both have nonsigmoidal (linear or exponential) dependencies on GdnHCl concentration. Indeed, several equilibrium unfolding studies, using ensemble[66,76−78] or single-molecule[79] measurements, as well as a kinetic unfolding study,[80] have suggested that protein unfolding reactions may be gradual in nature.

Conformational Interconversion within the I_U Ensemble. The transition from N to I_U happens in a burst phase lasting a few milliseconds, and all molecules have formed I_U at the end of this burst phase when unfolding is conducted at GdnHCl concentrations of >3 M (see above). Nevertheless, the hyperfluorescence of W53 in I_U keeps increasing in a monotonically linear manner with an increase in GdnHCl concentration above 3 M (Figure 4A,B). The increase in the fluorescence of W53 in I_U with an increase in GdnHCl concentration is substantially greater than the increase in fluorescence of NATA with an increase in GdnHCl concentration. This observation suggests the structure of I_U changes in a gradual manner with an increase in GdnHCl concentration, such that W53 becomes more secluded from solvent in I_U at higher GdnHCl concentrations. This would lead to an increase in the quantum yield of the fluorescence of W53 in I_U at high GdnHCl concentrations. It is likely that I_U is itself an ensemble of conformations differing in the extent to which W53 is buried, and that increasing the GdnHCl concentration results a shift in the population distribution

dx.doi.org/10.1021/bi3008627 | Biochemistry 2012, 51, 8226−8234

within the ensemble and leads to the preferential population of conformations in which W53 is more buried. Such solvent-induced tuning of structure has been observed previously in folding intermediates.[5,59,62,81]

Significance of This Study. It has been shown previously that I_U forms after the rate-limiting step, during the folding of the PI3K SH3 domain.[50] Hence, it appears that the non-native structure involving the partial burial of W53 in I_U persists very late into the folding reaction. It will be important in future studies to determine whether the non-native interaction of W53 is specific or nonspecific in terms of its partnering residues, whether it plays a role in stabilizing I_U, and whether it plays a critical role in completing the folding process.

Non-native interactions may play a critical role in driving the conformational change that functionally activates a protein, and they may act as a safeguard against complete unfolding of the protein during such activation.[82] However, they may also have adverse effects. For example, non-native interactions have been implicated in driving the aggregation of the yeast prion protein.[83] In general, they may lead to the transient exposure of aggregation-prone regions of a protein.[23] Partially unfolded forms of proteins, especially those possessing non-native interactions, have a tendency to aggregate,[48] including into amyloid aggregates.[84] It remains to be determined whether the transient burial of W53 in a hydrophobic pocket, driven by non-native interactions, plays a role in amyloid fibril formation by the PI3K SH3 domain.

AUTHOR INFORMATION

Corresponding Author

*E-mail: jayant@ncbs.res.in. Phone: 91-80-23666150. Fax: 91-80-23636662.

Funding

J.B.U. is the recipient of a J. C. Bose National Fellowship from the Government of India. This work was funded by the Tata Institute of Fundamental Research and by the Department of Science and Technology, Government of India.

Notes

The authors declare no competing financial interest.

ACKNOWLEDGMENTS

We thank members of our laboratory for discussions and Dr. Shachi Gosavi for her comments on the manuscript.

ABBREVIATIONS

ANS, 1-anilinonaphthalene-8-sulfonate; PI3K SH3 domain, SH3 domain of PI3 kinase.

REFERENCES

(1) Evans, P. A., Topping, K. D., Woolfson, D. N., and Dobson, C. M. (1991) Hydrophobic clustering in nonnative states of a protein: Interpretation of chemical shifts in NMR spectra of denatured states of lysozyme. *Proteins 9*, 248−266.

(2) Mok, Y. K., Kay, C. M., Kay, L. E., and Forman-Kay, J. (1999) NOE data demonstrating a compact unfolded state for an SH3 domain under non-denaturing conditions. *J. Mol. Biol. 289*, 619−638.

(3) Bai, Y., Chung, J., Dyson, H. J., and Wright, P. E. (2001) Structural and dynamic characterization of an unfolded state of poplar apo-plastocyanin formed under nondenaturing conditions. *Protein Sci. 10*, 1056−1066.

(4) Bhavesh, N. S., Juneja, J., Udgaonkar, J. B., and Hosur, R. V. (2004) Native and nonnative conformational preferences in the urea-unfolded state of barstar. *Protein Sci. 13*, 3085−3091.

(5) Pradeep, L., and Udgaonkar, J. B. (2004) Effect of salt on the urea-unfolded form of barstar probed by m value measurements. *Biochemistry 43*, 11393−11402.

(6) Nabuurs, S. M., de Kort, B. J., Westphal, A. H., and van Mierlo, C. P. (2010) Non-native hydrophobic interactions detected in unfolded apoflavodoxin by paramagnetic relaxation enhancement. *Eur. Biophys. J. 39*, 689−698.

(7) Rothwarf, D. M., and Scheraga, H. A. (1996) Role of non-native aromatic and hydrophobic interactions in the folding of hen egg white lysozyme. *Biochemistry 35*, 13797−13807.

(8) Kuwata, K., Shastry, R., Cheng, H., Hoshino, M., Batt, C. A., Goto, Y., and Roder, H. (2001) Structural and kinetic characterization of early folding events in β-lactoglobulin. *Nat. Struct. Biol. 8*, 151−155.

(9) Wang, Y., and Shortle, D. (1995) The equilibrium folding pathway of staphylococcal nuclease: Identification of the most stable chain-chain interactions by NMR and CD spectroscopy. *Biochemistry 34*, 15895−15905.

(10) Crowhurst, K. A., Tollinger, M., and Forman-Kay, J. D. (2002) Cooperative interactions and a non-native buried Trp in the unfolded state of an SH3 domain. *J. Mol. Biol. 322*, 163−178.

(11) Klein-Seetharaman, J., Oikawa, M., Grimshaw, S. B., Wirmer, J., Duchardt, E., Ueda, T., Imoto, T., Smith, L. J., Dobson, C. M., and Schwalbe, H. (2002) Long-range interactions within a nonnative protein. *Science 295*, 1719−1722.

(12) Baum, J., Dobson, C. M., Evans, P. A., and Hanley, C. (1989) Characterization of a partly folded protein by NMR methods: Studies on the molten globule state of guinea pig α-lactalbumin. *Biochemistry 28*, 7−13.

(13) Balbach, J., Forge, V., Lau, W. S., Jones, J. A., van Nuland, N. A., and Dobson, C. M. (1997) Detection of residue contacts in a protein folding intermediate. *Proc. Natl. Acad. Sci. U.S.A. 94*, 7182−7185.

(14) Kuwajima, K., Yamaya, H., Miwa, S., Sugai, S., and Nagamura, T. (1987) Rapid formation of secondary structure framework in protein folding studied by stopped-flow circular dichroism. *FEBS Lett. 221*, 115−118.

(15) Hamada, D., Segawa, S., and Goto, Y. (1996) Non-native α-helical intermediate in the refolding of β-lactoglobulin, a predominantly β-sheet protein. *Nat. Struct. Biol. 3*, 868−873.

(16) Mizuguchi, M., Masaki, K., and Nitta, K. (1999) The molten globule state of a chimera of human α-lactalbumin and equine lysozyme. *J. Mol. Biol. 292*, 1137−1148.

(17) Capaldi, A. P., Kleanthous, C., and Radford, S. E. (2002) Im7 folding mechanism: Misfolding on a path to the native state. *Nat. Struct. Biol. 9*, 209−216.

(18) Feng, H., Takei, J., Lipsitz, R., Tjandra, N., and Bai, Y. (2003) Specific non-native hydrophobic interactions in a hidden folding intermediate: Implications for protein folding. *Biochemistry 42*, 12461−12465.

(19) Mason, J. M., Cliff, M. J., Sessions, R. B., and Clarke, A. R. (2005) Low energy pathways and non-native interactions: The influence of artificial disulfide bridges on the mechanism of folding. *J. Biol. Chem. 280*, 40494−40499.

(20) Neudecker, P., Zarrine-Afsar, A., Choy, W. Y., Muhandiram, D. R., Davidson, A. R., and Kay, L. E. (2006) Identification of a collapsed intermediate with non-native long-range interactions on the folding pathway of a pair of Fyn SH3 domain mutants by NMR relaxation dispersion spectroscopy. *J. Mol. Biol. 363*, 958−976.

(21) Nishimura, C., Dyson, H. J., and Wright, P. E. (2006) Identification of native and non-native structure in kinetic folding intermediates of apomyoglobin. *J. Mol. Biol. 355*, 139−156.

(22) Li, J., Shinjo, M., Matsumura, Y., Morita, M., Baker, D., Ikeguchi, M., and Kihara, H. (2007) An α-helical burst in the src SH3 folding pathway. *Biochemistry 46*, 5072−5082.

(23) Neudecker, P., Robustelli, P., Cavalli, A., Walsh, P., Lundstrom, P., Zarrine-Afsar, A., Sharpe, S., Vendruscolo, M., and Kay, L. E. (2012) Structure of an intermediate state in protein folding and aggregation. *Science 336*, 362−366.

(24) Sakurai, K., Fujioka, S., Konuma, T., Yagi, M., and Goto, Y. (2011) A circumventing role for the non-native intermediate in the folding of β-lactoglobulin. *Biochemistry 50*, 6498−6507.
(25) Fersht, A. R. (1995) Characterizing transition states in protein folding: An essential step in the puzzle. *Curr. Opin. Struct. Biol. 5*, 79−84.
(26) Martinez, J. C., Pisabarro, M. T., and Serrano, L. (1998) Obligatory steps in protein folding and the conformational diversity of the transition state. *Nat. Struct. Biol. 5*, 721−729.
(27) Martinez, J. C., and Serrano, L. (1999) The folding transition state between SH3 domains is conformationally restricted and evolutionarily conserved. *Nat. Struct. Biol. 6*, 1010−1016.
(28) Zarrine-Afsar, A., Dahesh, S., and Davidson, A. R. (2012) A residue in helical conformation in the native state adopts a β-strand conformation in the folding transition state despite its high and canonical φ-value. *Proteins 80*, 1343−1349.
(29) Li, L., Mirny, L. A., and Shakhnovich, E. I. (2000) Kinetics, thermodynamics and evolution of non-native interactions in a protein folding nucleus. *Nat. Struct. Biol. 7*, 336−342.
(30) Zarrine-Afsar, A., Wallin, S., Neculai, A. M., Neudecker, P., Howell, P. L., Davidson, A. R., and Chan, H. S. (2008) Theoretical and experimental demonstration of the importance of specific nonnative interactions in protein folding. *Proc. Natl. Acad. Sci. U.S.A. 105*, 9999−10004.
(31) Go, N. (1983) Theoretical studies of protein folding. *Annu. Rev. Biophys. Bioeng. 12*, 183−210.
(32) Jackson, S. E., and Fersht, A. R. (1991) Folding of chymotrypsin inhibitor 2. 1. Evidence for a two-state transition. *Biochemistry 30*, 10428−10435.
(33) Plaxco, K. W., Simons, K. T., and Baker, D. (1998) Contact order, transition state placement and the refolding rates of single domain proteins. *J. Mol. Biol. 277*, 985−994.
(34) Kaya, H., and Chan, H. S. (2003) Solvation effects and driving forces for protein thermodynamic and kinetic cooperativity: How adequate is native-centric topological modeling? *J. Mol. Biol. 326*, 911−931.
(35) Bowman, G. R., Voelz, V. A., and Pande, V. S. (2011) Taming the complexity of protein folding. *Curr. Opin. Struct. Biol. 21*, 4−11.
(36) Yoo, T. Y., Adhikari, A., Xia, Z., Huynh, T., Freed, K. F., Zhou, R., and Sosnick, T. R. (2012) The Folding Transition State of Protein L Is Extensive with Nonnative Interactions (and Not Small and Polarized). *J. Mol. Biol. 420*, 220−234.
(37) Clementi, C., and Plotkin, S. S. (2004) The effects of nonnative interactions on protein folding rates: Theory and simulation. *Protein Sci. 13*, 1750−1766.
(38) Das, P., Wilson, C. J., Fossati, G., Wittung-Stafshede, P., Matthews, K. S., and Clementi, C. (2005) Characterization of the folding landscape of monomeric lactose repressor: Quantitative comparison of theory and experiment. *Proc. Natl. Acad. Sci. U.S.A. 102*, 14569−14574.
(39) Gin, B. C., Garrahan, J. P., and Geissler, P. L. (2009) The limited role of nonnative contacts in the folding pathways of a lattice protein. *J. Mol. Biol. 392*, 1303−1314.
(40) Faisca, P. F., Nunes, A., Travasso, R. D., and Shakhnovich, E. I. (2010) Non-native interactions play an effective role in protein folding dynamics. *Protein Sci. 19*, 2196−2209.
(41) Englander, S. W. (2000) Protein folding intermediates and pathways studied by hydrogen exchange. *Annu. Rev. Biophys. Biomol. Struct. 29*, 213−238.
(42) Juneja, J., and Udgaonkar, J. B. (2002) Characterization of the unfolding of ribonuclease a by a pulsed hydrogen exchange study: Evidence for competing pathways for unfolding. *Biochemistry 41*, 2641−2654.
(43) Wani, A. H., and Udgaonkar, J. B. (2009) Native state dynamics drive the unfolding of the SH3 domain of PI3 kinase at high denaturant concentration. *Proc. Natl. Acad. Sci. U.S.A. 106*, 20711−20716.
(44) Zaidi, F. N., Nath, U., and Udgaonkar, J. B. (1997) Multiple intermediates and transition states during protein unfolding. *Nat. Struct. Biol. 4*, 1016−1024.
(45) Rami, B. R., and Udgaonkar, J. B. (2001) pH-jump-induced folding and unfolding studies of barstar: Evidence for multiple folding and unfolding pathways. *Biochemistry 40*, 15267−15279.
(46) Sridevi, K., and Udgaonkar, J. B. (2002) Unfolding rates of barstar determined in native and low denaturant conditions indicate the presence of intermediates. *Biochemistry 41*, 1568−1578.
(47) Borgia, A., Bonivento, D., Travaglini-Allocatelli, C., Di Matteo, A., and Brunori, M. (2006) Unveiling a hidden folding intermediate in c-type cytochromes by protein engineering. *J. Biol. Chem. 281*, 9331−9336.
(48) Wani, A. H., and Udgaonkar, J. B. (2006) HX-ESI-MS and optical studies of the unfolding of thioredoxin indicate stabilization of a partially unfolded, aggregation-competent intermediate at low pH. *Biochemistry 45*, 11226−11238.
(49) Patra, A. K., and Udgaonkar, J. B. (2007) Characterization of the folding and unfolding reactions of single-chain monellin: Evidence for multiple intermediates and competing pathways. *Biochemistry 46*, 11727−11743.
(50) Wani, A. H., and Udgaonkar, J. B. (2009) Revealing a concealed intermediate that forms after the rate-limiting step of refolding of the SH3 domain of PI3 kinase. *J. Mol. Biol. 387*, 348−362.
(51) Hoeltzli, S. D., and Frieden, C. (1995) Stopped-flow NMR spectroscopy: Real-time unfolding studies of 6-^{19}F-tryptophan-labeled *Escherichia coli* dihydrofolate reductase. *Proc. Natl. Acad. Sci. U.S.A. 92*, 9318−9322.
(52) Guijarro, J. I., Sunde, M., Jones, J. A., Campbell, I. D., and Dobson, C. M. (1998) Amyloid fibril formation by an SH3 domain. *Proc. Natl. Acad. Sci. U.S.A. 95*, 4224−4228.
(53) Bayro, M. J., Maly, T., Birkett, N. R., Macphee, C. E., Dobson, C. M., and Griffin, R. G. (2010) High-resolution MAS NMR analysis of PI3-SH3 amyloid fibrils: Backbone conformation and implications for protofilament assembly and structure. *Biochemistry 49*, 7474−7484.
(54) Dasgupta, A., and Udgaonkar, J. B. (2010) Evidence for initial non-specific polypeptide chain collapse during the refolding of the SH3 domain of PI3 kinase. *J. Mol. Biol. 403*, 430−445.
(55) Bader, R., Bamford, R., Zurdo, J., Luisi, B. F., and Dobson, C. M. (2006) Probing the mechanism of amyloidogenesis through a tandem repeat of the PI3-SH3 domain suggests a generic model for protein aggregation and fibril formation. *J. Mol. Biol. 356*, 189−208.
(56) Lee, B., and Richards, F. M. (1971) The interpretation of protein structures: Estimation of static accessibility. *J. Mol. Biol. 55*, 379−400.
(57) Stryer, L. (1965) The interaction of a naphthalene dye with apomyoglobin and apohemoglobin. A fluorescent probe of non-polar binding sites. *J. Mol. Biol. 13*, 482−495.
(58) Kiefhaber, T., Schmid, F. X., Willaert, K., Engelborghs, Y., and Chaffotte, A. (1992) Structure of a rapidly formed intermediate in ribonuclease T1 folding. *Protein Sci. 1*, 1162−1172.
(59) Pradeep, L., and Udgaonkar, J. B. (2002) Differential salt-induced stabilization of structure in the initial folding intermediate ensemble of barstar. *J. Mol. Biol. 324*, 331−347.
(60) Park, S. H. (2004) Hydrophobic core variant ubiquitin forms a molten globule conformation at acidic pH. *J. Biochem. Mol. Biol. 37*, 676−683.
(61) Guijarro, J. I., Morton, C. J., Plaxco, K. W., Campbell, I. D., and Dobson, C. M. (1998) Folding kinetics of the SH3 domain of PI3 kinase by real-time NMR combined with optical spectroscopy. *J. Mol. Biol. 276*, 657−667.
(62) Dasgupta, A., and Udgaonkar, J. B. (2012) Four-State Folding of a SH3 Domain: Salt-Induced Modulation of the Stabilities of the Intermediates and Native State. *Biochemistry 51*, 4723−4734.
(63) Ptitsyn, O. B. (1995) Molten globule and protein folding. *Adv. Protein Chem. 47*, 83−229.
(64) Semisotnov, G. V., Rodionova, N. A., Razgulyaev, O. I., Uversky, V. N., Gripas, A. F., and Gilmanshin, R. I. (1991) Study of the "molten

globule" intermediate state in protein folding by a hydrophobic fluorescent probe. *Biopolymers 31*, 119−128.
(65) Sherman, M. A., Beechem, J. M., and Mas, M. T. (1995) Probing intradomain and interdomain conformational changes during equilibrium unfolding of phosphoglycerate kinase: Fluorescence and circular dichroism study of tryptophan mutants. *Biochemistry 34*, 13934−13942.
(66) Swaminathan, R., Nath, U., Udgaonkar, J. B., Periasamy, N., and Krishnamoorthy, G. (1996) Motional dynamics of a buried tryptophan reveals the presence of partially structured forms during denaturation of barstar. *Biochemistry 35*, 9150−9157.
(67) Chen, Y., and Barkley, M. D. (1998) Toward understanding tryptophan fluorescence in proteins. *Biochemistry 37*, 9976−9982.
(68) Schmid, F. X. (1997) Optical spectroscopy to characterize protein conformation and conformational changes. In *Protein structure: A practical approach* (Creighton, T. E., Ed.) pp 261−297, Oxford University Press, New York.
(69) Eftink, M. R., and Lakowicz, J. R. (2002) Intrinsic Fluorescence of Proteins. In *Topics in Fluorescence Spectroscopy* (Geddes, C. D., and Lakowicz, J. R., Eds.) pp 1−15, Springer, New York.
(70) Schuler, B., Lipman, E. A., and Eaton, W. A. (2002) Probing the free-energy surface for protein folding with single-molecule fluorescence spectroscopy. *Nature 419*, 743−747.
(71) Sinha, K. K., and Udgaonkar, J. B. (2005) Dependence of the size of the initially collapsed form during the refolding of barstar on denaturant concentration: Evidence for a continuous transition. *J. Mol. Biol. 353*, 704−718.
(72) Sadqi, M., Fushman, D., and Munoz, V. (2006) Atom-by-atom analysis of global downhill protein folding. *Nature 442*, 317−321.
(73) Jha, S. K., and Udgaonkar, J. B. (2007) Exploring the cooperativity of the fast folding reaction of a small protein using pulsed thiol labeling and mass spectrometry. *J. Biol. Chem. 282*, 37479−37491.
(74) Sinha, K. K., and Udgaonkar, J. B. (2007) Dissecting the non-specific and specific components of the initial folding reaction of barstar by multi-site FRET measurements. *J. Mol. Biol. 370*, 385−405.
(75) Sinha, K. K., and Udgaonkar, J. B. (2008) Barrierless evolution of structure during the submillisecond refolding reaction of a small protein. *Proc. Natl. Acad. Sci. U.S.A. 105*, 7998−8003.
(76) Lakshmikanth, G. S., Sridevi, K., Krishnamoorthy, G., and Udgaonkar, J. B. (2001) Structure is lost incrementally during the unfolding of barstar. *Nat. Struct. Biol. 8*, 799−804.
(77) Oliva, F. Y., and Munoz, V. (2004) A simple thermodynamic test to discriminate between two-state and downhill folding. *J. Am. Chem. Soc. 126*, 8596−8597.
(78) Ahmed, Z., Beta, I. A., Mikhonin, A. V., and Asher, S. A. (2005) UV-resonance Raman thermal unfolding study of Trp-cage shows that it is not a simple two-state miniprotein. *J. Am. Chem. Soc. 127*, 10943−10950.
(79) Kuzmenkina, E. V., Heyes, C. D., and Nienhaus, G. U. (2006) Single-molecule FRET study of denaturant induced unfolding of RNase H. *J. Mol. Biol. 357*, 313−324.
(80) Jha, S. K., Dhar, D., Krishnamoorthy, G., and Udgaonkar, J. B. (2009) Continuous dissolution of structure during the unfolding of a small protein. *Proc. Natl. Acad. Sci. U.S.A. 106*, 11113−11118.
(81) Sridevi, K., Lakshmikanth, G. S., Krishnamoorthy, G., and Udgaonkar, J. B. (2004) Increasing stability reduces conformational heterogeneity in a protein folding intermediate ensemble. *J. Mol. Biol. 337*, 699−711.
(82) Gardino, A. K., Villali, J., Kivenson, A., Lei, M., Liu, C. F., Steindel, P., Eisenmesser, E. Z., Labeikovsky, W., Wolf-Watz, M., Clarkson, M. W., and Kern, D. (2009) Transient non-native hydrogen bonds promote activation of a signaling protein. *Cell 139*, 1109−1118.
(83) Ohhashi, Y., Ito, K., Toyama, B. H., Weissman, J. S., and Tanaka, M. (2010) Differences in prion strain conformations result from non-native interactions in a nucleus. *Nat. Chem. Biol. 6*, 225−230.
(84) Chiti, F., and Dobson, C. M. (2009) Amyloid formation by globular proteins under native conditions. *Nat. Chem. Biol. 5*, 15−22.
(85) Pettersen, E. F., Goddard, T. D., Huang, C. C., Couch, G. S., Greenblatt, D. M., Meng, E. C., and Ferrin, T. E. (2004) UCSF Chimera: A visualization system for exploratory research and analysis. *J. Comput. Chem. 25*, 1605−1612.